Lyapunov-Function-Based Flux and Speed Observer for AC Induction Motor Sensorless Control and Parameters Estimation

Pavel Vaclavek, *Member, IEEE*, and Petr Blaha

***Abstract*—AC induction motors have become very popular for motion-control applications due to their simple and reliable construction. Control of drives based on ac induction motors is a quite complex task. Provided the vector-control algorithm is used, not only the rotor speed but also the position of the magnetic flux inside the motor during the control process should be known. In most applications, the flux sensors are omitted and the magnetic-flux phasor position has to be calculated. However, there are also applications in which even speed sensors should be omitted. In such a situation, the task of state reconstruction can be solved only from voltage and current measurements. In the current paper, a method based on deterministic evaluation of measurement using the state observer based on the Lyapunov function is presented. The method has been proven in testing on a real ac induction machine.**

***Index Terms*—AC motor drives, Lyapunov methods, nonlinear systems, observers.**

I. Introduction

INDUCTION motors have become more and more popular due to their reliable construction. If we intend to use an ac induction motor in a low-cost application (e.g., mass-produced washing machine), it is necessary to optimize production costs. Many applications require precise speed control. The speed sensor is quite an expensive device compared to other parts of the drive. That is why we are trying to develop a reliable control system that estimates the rotor speed from electrical quantities instead of using a speed sensor. The idea of using a state observer for evaluation of the signals needed for ac induction-motor control is known [1]–[3]. In most cases, such applications exploit the Kalman-filter algorithm to estimate the values of states that cannot be measured directly [4]. The Kalman filter provides a unified method for the state-observer design, and that is why it is relatively easy to use. Another possibility is to find a state observer fitted exactly for the drive. It is possible to use a simple structure similar to Luenberger's observer with many advantages, e.g., low computational demands and results similar to the Kalman-filter algorithm [5], [6].

Manuscript received May 25, 2004; revised November 23, 2004. Abstract published on the Internet November 25, 2005. This work was supported by the Ministry of Education of the Czech Republic under Project 1M0567 "Center for Applied Cybernetics," by the Czech Science Foundation under Project 102/06/0949, and by Freescale Semiconductor Czech Republic (former division of Motorola).

The authors are with the Center for Applied Cybernetics, Brno University of Technology, Brno 61200, Czech Republic (e-mail: vaclavek@feec.vutbr.cz; blahap@feec.vutbr.cz).

Digital Object Identifier 10.1109/TIE.2005.862305

The algorithms need an accurate model of the controlled drive to compute a good estimate of unknown state variables. The parameters, especially resistances, can change dramatically during the drive operation because of working-temperature changes. There are some methods for ac induction-machine-parameter estimation [7]. It would be very useful if the observer algorithm could also directly estimate some of the ac induction-drive parameters. Another problem is the observer stability. In this paper, we are trying to present observer design that should guarantee the algorithm stability.

A. AC Induction-Motor Model

There are many models of ac induction motors. We use the so-called t-model structure, known also as Kovacs model

$$\frac{d\boldsymbol{\Psi}_\mathrm{s}}{dt} = \boldsymbol{u}_\mathrm{s} - R_\mathrm{s}\boldsymbol{i}_\mathrm{s} \tag{1}$$

$$\frac{d\boldsymbol{\Psi}_\mathrm{r}}{dt} = jz_\mathrm{p}\omega\boldsymbol{\Psi}_\mathrm{r} - R_\mathrm{r}\boldsymbol{i}_\mathrm{r} \tag{2}$$

$$\frac{d\omega}{dt} = \frac{1}{J}(T - T_\mathrm{load}) \tag{3}$$

$$\boldsymbol{\Psi}_\mathrm{s} = L_\mathrm{s}\boldsymbol{i}_\mathrm{s} + L_\mathrm{m}\boldsymbol{i}_\mathrm{r} \tag{4}$$

$$\boldsymbol{\Psi}_\mathrm{r} = L_\mathrm{m}\boldsymbol{i}_\mathrm{s} + L_\mathrm{r}\boldsymbol{i}_\mathrm{r} \tag{5}$$

$$T = 1.5z_\mathrm{p}\Im(\overline{\boldsymbol{\Psi}}_\mathrm{s}\boldsymbol{i}_\mathrm{s}) \tag{6}$$

where $\boldsymbol{\Psi}_\mathrm{s} = \Psi_{\mathrm{s}\alpha} + j\Psi_{\mathrm{s}\beta}$, $\boldsymbol{\Psi}_\mathrm{r} = \Psi_{\mathrm{r}\alpha} + j\Psi_{\mathrm{r}\beta}$ are the stator and rotor magnetic-flux phasors in $\alpha\beta$ coordinates; $\boldsymbol{u}_\mathrm{s} = u_{\mathrm{s}\alpha} + ju_{\mathrm{s}\beta}$ is the stator-voltage phasor; $\boldsymbol{i}_\mathrm{s} = i_{\mathrm{s}\alpha} + ji_{\mathrm{s}\beta}$, $\boldsymbol{i}_\mathrm{r} = i_{\mathrm{r}\alpha} + ji_{\mathrm{r}\beta}$ are the stator and rotor current phasors; ω is the rotor angular velocity; T, T_load are the driving and load torques; R_s, R_r are the stator and rotor resistances; z_p is the number of pole pairs; J is the rotor inertia; and L_s, L_r, L_m are the inductances.

As the load torque and the rotor inertia are not usually known, it is not possible to use (3) and (6). The remaining equations can be, after some computations, transferred into a more suitable form

$$\frac{d\boldsymbol{i}'_\mathrm{s}}{dt} = \boldsymbol{u}_\mathrm{s} - \xi_1\boldsymbol{i}'_\mathrm{s} + \boldsymbol{\Psi}'_\mathrm{r}(\xi_2 - j\omega z_\mathrm{p}) \tag{7}$$

$$\frac{d\boldsymbol{\Psi}'_\mathrm{r}}{dt} = \xi_3\boldsymbol{i}'_\mathrm{s} - \boldsymbol{\Psi}'_\mathrm{r}(\xi_2 - j\omega z_\mathrm{p}) \tag{8}$$

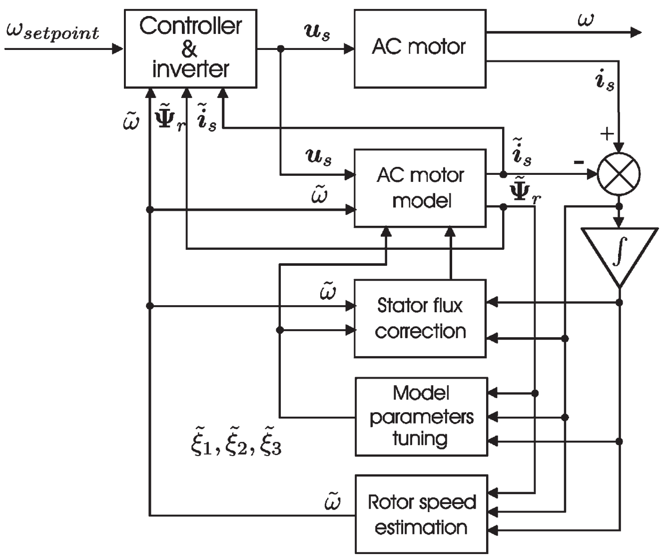

Fig. 1. Speed and flux observer structure.

where

$$\boldsymbol{i}'_{\rm s} = \boldsymbol{i}_{\rm s}\frac{L_{\rm s}L_{\rm r} - L_{\rm m}^2}{L_{\rm r}} \tag{9}$$

$$\boldsymbol{\Psi}'_{\rm r} = \boldsymbol{\Psi}_{\rm r}\frac{L_{\rm m}}{L_{\rm r}} \tag{10}$$

$$\xi_1 = \frac{R_{\rm s}L_{\rm r}^2 + R_{\rm r}L_{\rm m}^2}{L_{\rm s}L_{\rm r}^2 - L_{\rm r}L_{\rm m}^2} \tag{11}$$

$$\xi_2 = \frac{R_{\rm r}}{L_{\rm r}} \tag{12}$$

$$\xi_3 = R_{\rm r}\frac{L_{\rm m}^2}{L_{\rm s}L_{\rm r}^2 - L_{\rm r}L_{\rm m}^2}. \tag{13}$$

Equations (7) and (8) represent some kind of model normalized according to the motor inductances. The model has only three independent parameters ξ_1, ξ_2, and ξ_3. It is clear that inductances also have to be known to use (9)–(13), but it is not usually a problem. Inductances can be measured offline and we can suppose that they do not change significantly during normal drive operation.

II. State Observer

The used control structure is shown in Fig. 1. The state observer can use measurement of stator voltage and modified current $\boldsymbol{u}_{\rm s}$ and $\boldsymbol{i}'_{\rm s}$. It should estimate modified rotor magnetic flux $\boldsymbol{\Psi}'_{\rm r}$, rotor angular velocity ω, modified stator current $\boldsymbol{i}'_{\rm s}$ (filtering purposes), and, if possible, also parameters ξ_1, ξ_2, and ξ_3. Let us suppose an estimator structure in the form

$$\frac{d\tilde{\boldsymbol{i}}'_{\rm s}}{dt} = \boldsymbol{u}_{\rm s} - \tilde{\xi}_1\tilde{\boldsymbol{i}}'_{\rm s} + \tilde{\boldsymbol{\Psi}}'_{\rm r}(\tilde{\xi}_2 - j\tilde{\omega}z_{\rm p}) + \boldsymbol{\delta} \tag{14}$$

$$\frac{d\tilde{\boldsymbol{\Psi}}'_{\rm r}}{dt} = \tilde{\xi}_3\tilde{\boldsymbol{i}}'_{\rm s} - \tilde{\boldsymbol{\Psi}}'_{\rm r}(\tilde{\xi}_2 - j\tilde{\omega}z_{\rm p}) \tag{15}$$

where $\tilde{x}$ stands for the estimate of variable x, and $\boldsymbol{\delta}$ is a correction based on the estimated and measured stator current.

We can define error functions describing the difference between real and estimated values of the variables

$$\Delta\boldsymbol{i}'_{\rm s} = \tilde{\boldsymbol{i}}'_{\rm s} - \boldsymbol{i}'_{\rm s} \tag{16}$$

$$\Delta\boldsymbol{\Psi}'_{\rm r} = \tilde{\boldsymbol{\Psi}}'_{\rm r} - \boldsymbol{\Psi}'_{\rm r} \tag{17}$$

$$\Delta\omega = \tilde{\omega} - \omega \tag{18}$$

$$\Delta\xi_1 = \tilde{\xi}_1 - \xi_1 \tag{19}$$

$$\Delta\xi_2 = \tilde{\xi}_2 - \xi_2 \tag{20}$$

$$\Delta\xi_3 = \tilde{\xi}_3 - \xi_3. \tag{21}$$

From (16) and (17), we can get

$$\frac{d\Delta\boldsymbol{i}'_{\rm s}}{dt} = \frac{d\tilde{\boldsymbol{i}}'_{\rm s}}{dt} - \frac{d\boldsymbol{i}'_{\rm s}}{dt} \tag{22}$$

$$\frac{d\Delta\boldsymbol{\Psi}'_{\rm r}}{dt} = \frac{d\tilde{\boldsymbol{\Psi}}'_{\rm r}}{dt} - \frac{d\boldsymbol{\Psi}'_{\rm r}}{dt} \tag{23}$$

and after substitution of (7) and (14) into (22) and (8) and (15) into (23)

$$\begin{aligned}\frac{d\Delta\boldsymbol{i}'_{\rm s}}{dt} =& (\Delta\xi_2 - jz_{\rm p}\Delta\omega)\tilde{\boldsymbol{\Psi}}'_{\rm r} - \Delta\boldsymbol{i}'_{\rm s}\tilde{\xi}_1 - \boldsymbol{i}'_{\rm s}\Delta\xi_1 \\ &+ \left(jz_{\rm p}(\Delta\omega - \tilde{\omega}) - \Delta\xi_2 + \tilde{\xi}_2\right)\Delta\boldsymbol{\Psi}'_{\rm r} + \boldsymbol{\delta}\end{aligned} \tag{24}$$

$$\begin{aligned}\frac{d\Delta\boldsymbol{\Psi}'_{\rm r}}{dt} =& -(\Delta\xi_2 - jz_{\rm p}\Delta\omega)\tilde{\boldsymbol{\Psi}}'_{\rm r} + \Delta\boldsymbol{i}'_{\rm s}\tilde{\xi}_3 + \boldsymbol{i}'_{\rm s}\Delta\xi_3 \\ &- \left(jz_{\rm p}(\Delta\omega - \tilde{\omega}) - \Delta\xi_2 + \tilde{\xi}_2\right)\Delta\boldsymbol{\Psi}'_{\rm r}.\end{aligned} \tag{25}$$

Equations (24) and (25) represent a dynamical system of estimation errors. We will try to find such correction $\boldsymbol{\delta}$ that will minimize estimation errors. Also, the best possible coincidence of the model and the real system is achieved when

$$\Delta\boldsymbol{i}'_{\rm s} = 0. \tag{26}$$

It is possible to transfer the task of estimation-error minimization to the task of solving the estimation-error dynamic-system stability. We can state

$$\frac{d\boldsymbol{x}'}{dt} = \Delta\boldsymbol{i}'_{\rm s} \tag{27}$$

where $\boldsymbol{x}'$ is an auxiliary state variable. It is clear that if (27) is stable, then (26) is valid. The system (27) can be stabilized if it has the form

$$\frac{d\boldsymbol{x}'}{dt} = \boldsymbol{y} - k_1\boldsymbol{x}' \tag{28}$$

where $\boldsymbol{y}$ is another auxiliary state variable that should go to 0. Now, we have to solve problem of stabilizing state variable $\boldsymbol{y}$.

This simple trick improves observer convergence as the current estimation error will go approximately exponentially to 0. Equations (27) and (28) lead to

$$\boldsymbol{y} = \Delta\boldsymbol{i}'_{\mathrm{s}} + k_1\boldsymbol{x}' \tag{29}$$

$$\frac{d\boldsymbol{y}}{dt} = \frac{d\Delta\boldsymbol{i}'_{\mathrm{s}}}{dt} + k_1\frac{d\boldsymbol{x}'}{dt} \tag{30}$$

and after substitution of (24) and (27) into (30), we will get

$$\begin{aligned}\frac{d\boldsymbol{y}}{dt} &= (\Delta\xi_2 - jz_{\mathrm{p}}\Delta\omega)\tilde{\boldsymbol{\Psi}}'_{\mathrm{r}} - \Delta\boldsymbol{i}'_{\mathrm{s}}\tilde{\xi}_1 - \boldsymbol{i}'_{\mathrm{s}}\Delta\xi_1\\ &\quad + \left(jz_{\mathrm{p}}(\Delta\omega - \tilde{\omega}) - \Delta\xi_2 + \tilde{\xi}_2\right)\Delta\boldsymbol{\Psi}'_{\mathrm{r}} + \delta + k_1\Delta\boldsymbol{i}'_{\mathrm{s}}.\end{aligned} \tag{31}$$

This method is sometimes called back-stepping control design. In the next step, the stability of the estimation-error dynamical system will be analyzed using the Lyapunov method. Let us suppose that the suitable Lyapunov function will be

$$\begin{aligned}V &= \frac{1}{2}|\boldsymbol{x}'|^2 + \frac{1}{2}|\boldsymbol{y}|^2 + \frac{1}{2}\left|\Delta\boldsymbol{\Psi}'_{\mathrm{r}}\right|^2\\ &\quad + \frac{1}{2}\frac{(\Delta\omega)^2}{k_\omega} + \frac{1}{2}\frac{(\Delta\xi_1)^2}{k_{\xi_1}} + \frac{1}{2}\frac{(\Delta\xi_2)^2}{k_{\xi_2}} + \frac{1}{2}\frac{(\Delta\xi_3)^2}{k_{\xi_3}}.\end{aligned} \tag{32}$$

The system will be stable if

$$\frac{dV}{dt} < 0 \tag{33}$$

for any combination of variable values. After a long calculation, it can be shown that if we put

$$\Delta\boldsymbol{\Psi}'_{\mathrm{r}} = -\Delta\boldsymbol{i}'_{\mathrm{s}} \tag{34}$$

$$\begin{aligned}\boldsymbol{\delta} &= (\tilde{\xi}_1 - k_1 - k_2)\Delta\boldsymbol{i}'_{\mathrm{s}}\\ &\quad + (jz_{\mathrm{p}}\tilde{\omega} - \tilde{\xi}_2)\Delta\boldsymbol{\Psi}'_{\mathrm{r}} - (1 + k_1k_2)\boldsymbol{x}'\end{aligned} \tag{35}$$

we will get

$$\begin{aligned}\frac{dV}{dt} &= -k_1|\boldsymbol{x}'|^2 - k_2|\boldsymbol{y}|^2 - \tilde{\xi}_2\left|\Delta\boldsymbol{\Psi}'_{\mathrm{r}}\right|^2 - \tilde{\xi}_3\left|\Delta\boldsymbol{i}'_{\mathrm{s}}\right|^2\\ &\quad + \left(\frac{\frac{d\Delta\omega}{dt}}{k_\omega} + \Im\left(\overline{(\boldsymbol{y} - \Delta\boldsymbol{\Psi}'_{\mathrm{r}})}\left(\tilde{\boldsymbol{\Psi}}'_{\mathrm{r}} - \Delta\boldsymbol{\Psi}'_{\mathrm{r}}\right)\right)\right)\Delta\omega\\ &\quad + \left(\frac{\frac{d\Delta\xi_1}{dt}}{k_{\xi_1}} - \Re\left(\boldsymbol{y}\overline{\boldsymbol{i}'_{\mathrm{s}}}\right)\right)\Delta\xi_1\\ &\quad + \left(\frac{\frac{d\Delta\xi_2}{dt}}{k_{\xi_2}} + \Re\left(\overline{(\boldsymbol{y} - \Delta\boldsymbol{\Psi}'_{\mathrm{r}})}\left(\tilde{\boldsymbol{\Psi}}'_{\mathrm{r}} - \Delta\boldsymbol{\Psi}'_{\mathrm{r}}\right)\right)\right)\Delta\xi_2\\ &\quad + \left(\frac{\frac{d\Delta\xi_3}{dt}}{k_{\xi_3}} + \Re\left(\Delta\boldsymbol{\Psi}'_{\mathrm{r}}\overline{\boldsymbol{i}'_{\mathrm{s}}}\right)\right)\Delta\xi_3.\end{aligned} \tag{36}$$

It is necessary to fulfill the following conditions to achieve the validity of (33):

$$k_1 > 0 \quad k_2 > 0 \quad \tilde{\xi}_2 > 0 \quad \tilde{\xi}_3 > 0 \tag{37}$$

$$\frac{\frac{d\Delta\omega}{dt}}{k_\omega} + \Im\left(\overline{(\boldsymbol{y} - \Delta\boldsymbol{\Psi}'_{\mathrm{r}})}\left(\tilde{\boldsymbol{\Psi}}'_{\mathrm{r}} - \Delta\boldsymbol{\Psi}'_{\mathrm{r}}\right)\right) = 0 \tag{38}$$

$$\frac{\frac{d\Delta\xi_1}{dt}}{k_{\xi_1}} - \Re\left(\boldsymbol{y}\overline{\boldsymbol{i}'_{\mathrm{s}}}\right) = 0 \tag{39}$$

$$\frac{\frac{d\Delta\xi_2}{dt}}{k_{\xi_2}} + \Re\left(\overline{(\boldsymbol{y} - \Delta\boldsymbol{\Psi}'_{\mathrm{r}})}\left(\tilde{\boldsymbol{\Psi}}'_{\mathrm{r}} - \Delta\boldsymbol{\Psi}'_{\mathrm{r}}\right)\right) = 0 \tag{40}$$

$$\frac{\frac{d\Delta\xi_3}{dt}}{k_{\xi_3}} + \Re\left(\Delta\boldsymbol{\Psi}'_{\mathrm{r}}\overline{\boldsymbol{i}'_{\mathrm{s}}}\right) = 0. \tag{41}$$

The condition (37) can be easily fulfilled as constants k_1 and k_2 are freely selectable, and estimated parameters $\tilde{\xi}_2$ and $\tilde{\xi}_3$ should be always positive as they represent transformed rotor resistance. The conditions (38)–(41) can be fulfilled by stating

$$\frac{d\Delta\omega}{dt} = -k_\omega\Im\left(\overline{(\boldsymbol{y} - \Delta\boldsymbol{\Psi}'_{\mathrm{r}})}\left(\tilde{\boldsymbol{\Psi}}'_{\mathrm{r}} - \Delta\boldsymbol{\Psi}'_{\mathrm{r}}\right)\right) \tag{42}$$

$$\frac{d\Delta\xi_1}{dt} = k_{\xi_1}\Re\left(\boldsymbol{y}\overline{\boldsymbol{i}'_{\mathrm{s}}}\right) \tag{43}$$

$$\frac{d\Delta\xi_2}{dt} = -k_{\xi_2}\Re\left(\overline{(\boldsymbol{y} - \Delta\boldsymbol{\Psi}'_{\mathrm{r}})}\left(\tilde{\boldsymbol{\Psi}}'_{\mathrm{r}} - \Delta\boldsymbol{\Psi}'_{\mathrm{r}}\right)\right) \tag{44}$$

$$\frac{d\Delta\xi_3}{dt} = -k_{\xi_3}\Re\left(\Delta\boldsymbol{\Psi}'_{\mathrm{r}}\overline{\boldsymbol{i}'_{\mathrm{s}}}\right) \tag{45}$$

and the state observer will be stable. Equations (42)–(45) can be used to construct adaptation rules for parameter estimations. The changes of ac induction-motor parameters including angular velocity are very slow in comparison with stator voltages and currents. That is why we can consider them to be constant and, thus,

$$\frac{d\Delta\omega}{dt} = \frac{d\tilde{\omega}}{dt} - \frac{d\omega}{dt} \approx \frac{d\tilde{\omega}}{dt} \tag{46}$$

$$\frac{d\Delta\xi_1}{dt} = \frac{d\tilde{\xi}_1}{dt} - \frac{d\xi_1}{dt} \approx \frac{d\tilde{\xi}_1}{dt} \tag{47}$$

$$\frac{d\Delta\xi_2}{dt} = \frac{d\tilde{\xi}_2}{dt} - \frac{d\xi_2}{dt} \approx \frac{d\tilde{\xi}_2}{dt} \tag{48}$$

$$\frac{d\Delta\xi_3}{dt} = \frac{d\tilde{\xi}_3}{dt} - \frac{d\xi_3}{dt} \approx \frac{d\tilde{\xi}_3}{dt}. \tag{49}$$

The adaptation rules are then

$$\frac{d\tilde{\omega}}{dt} = -k_\omega\Im\left(\overline{(\boldsymbol{y} - \Delta\boldsymbol{\Psi}'_{\mathrm{r}})}\left(\tilde{\boldsymbol{\Psi}}'_{\mathrm{r}} - \Delta\boldsymbol{\Psi}'_{\mathrm{r}}\right)\right) \tag{50}$$

$$\frac{d\tilde{\xi}_1}{dt} = k_{\xi_1}\Re\left(\boldsymbol{y}\overline{\boldsymbol{i}'_{\mathrm{s}}}\right) \tag{51}$$

$$\frac{d\tilde{\xi}_2}{dt} = -k_{\xi_2}\Re\left(\overline{(\boldsymbol{y} - \Delta\boldsymbol{\Psi}'_{\mathrm{r}})}\left(\tilde{\boldsymbol{\Psi}}'_{\mathrm{r}} - \Delta\boldsymbol{\Psi}'_{\mathrm{r}}\right)\right) \tag{52}$$

$$\frac{d\tilde{\xi}_3}{dt} = -k_{\xi_3}\Re\left(\Delta\boldsymbol{\Psi}'_{\mathrm{r}}\overline{\boldsymbol{i}'_{\mathrm{s}}}\right). \tag{53}$$

The rotor magnetic-flux estimation error $\Delta\boldsymbol{\Psi}'_{\rm r}$ is not known and cannot be measured. We have assumed that its value is equal to the negative value of modified stator-current estimation error (34). Let us suppose that modified stator-current and rotor magnetic-flux estimation errors are small and steady. Then

$$\frac{d\Delta\boldsymbol{i}'_{\rm s}}{dt} = jz_{\rm p}\tilde{\omega}\Delta\boldsymbol{i}'_{\rm s} \tag{54}$$

$$\frac{d\Delta\boldsymbol{\Psi}'_{\rm r}}{ddt} = jz_{\rm p}\tilde{\omega}\Delta\boldsymbol{\Psi}'_{\rm r} \tag{55}$$

$$\frac{d\Delta\boldsymbol{i}'_{\rm s}}{dt} + \frac{d\Delta\boldsymbol{\Psi}'_{\rm r}}{dt} = jz_{\rm p}\tilde{\omega}\left(\Delta\boldsymbol{i}'_{\rm s} + \Delta\boldsymbol{\Psi}'_{\rm r}\right). \tag{56}$$

Substitution of (24) and (25) into (56) leads to

$$\Delta\boldsymbol{i}'_{\rm s} + \Delta\boldsymbol{\Psi}'_{\rm r} = \frac{-j}{z_{\rm p}\tilde{\omega}}\left((\Delta\xi_3 - \Delta\xi_1)\tilde{\boldsymbol{i}}'_{\rm s} + (\tilde{\xi}_3 - \tilde{\xi}_1)\Delta\boldsymbol{i}'_{\rm s} + \delta\right) \tag{57}$$

and if the estimation errors are small, we can write

$$\Delta\boldsymbol{i}'_{\rm s} + \Delta\boldsymbol{\Psi}'_{\rm r} \approx 0 \tag{58}$$

$$\Delta\boldsymbol{\Psi}'_{\rm r} \approx -\Delta\boldsymbol{i}'_{\rm s} \tag{59}$$

which proves the assumption (34). The algorithm is only locally stable because we have to assume that the differences between real and estimated variable values are small. The complete algorithm can be summarized into the following equations:

$$\Delta\boldsymbol{i}'_{\rm s} = \tilde{\boldsymbol{i}}'_{\rm s} - \boldsymbol{i}'_{\rm s} \tag{60}$$

$$\frac{d\boldsymbol{x}'}{dt} = \Delta\boldsymbol{i}'_{\rm s} \tag{61}$$

$$\boldsymbol{y} = \Delta\boldsymbol{i}'_{\rm s} + k_1\boldsymbol{x}' \tag{62}$$

$$\boldsymbol{\delta} = (\tilde{\xi}_1 + \tilde{\xi}_2 - k_1 - k_2 - jz_{\rm p}\tilde{\omega})\Delta\boldsymbol{i}'_{\rm s} - (1 + k_1k_2)\boldsymbol{x}' \tag{63}$$

$$\frac{d\tilde{\boldsymbol{i}}'_{\rm s}}{dt} = \boldsymbol{u}_{\rm s} - \tilde{\xi}_1\tilde{\boldsymbol{i}}'_{\rm s} + \tilde{\boldsymbol{\Psi}}'_{\rm r}(\tilde{\xi}_2 - j\tilde{\omega}z_{\rm p}) + \boldsymbol{\delta} \tag{64}$$

$$\frac{d\boldsymbol{\Psi}'_{\rm r}}{dt} = \tilde{\xi}_3\tilde{\boldsymbol{i}}'_{\rm s} - \tilde{\boldsymbol{\Psi}}'_{\rm r}(\tilde{\xi}_2 - j\tilde{\omega}z_{\rm p}) \tag{65}$$

$$\frac{d\tilde{\omega}}{dt} = -k_\omega\Im\left(\overline{(\boldsymbol{y} + \Delta\boldsymbol{i}'_{\rm s})}\left(\tilde{\boldsymbol{\Psi}}'_{\rm r} + \Delta\boldsymbol{i}'_{\rm s}\right)\right) \tag{66}$$

$$\frac{d\tilde{\xi}_1}{dt} = k_{\xi_1}\Re(\boldsymbol{y}\overline{\tilde{\boldsymbol{i}}'_{\rm s}}) \tag{67}$$

$$\frac{d\tilde{\xi}_2}{dt} = -k_{\xi_2}\Re\left(\overline{(\boldsymbol{y} + \Delta\boldsymbol{i}'_{\rm s})}\left(\tilde{\boldsymbol{\Psi}}'_{\rm r} + \Delta\boldsymbol{i}'_{\rm s}\right)\right) \tag{68}$$

$$\frac{d\tilde{\xi}_3}{dt} = k_{\xi_3}\Re\left(\Delta\boldsymbol{i}'_{\rm s}\overline{\tilde{\boldsymbol{i}}'_{\rm s}}\right) \tag{69}$$

with respect to (9)–(13). The behavior of the algorithm can be tuned by a set of selectable parameters $\{k_1, k_2, k_\omega, k_{\xi_1}, k_{\xi_2}, k_{\xi_3}\}$.

A. Parameter Estimation

The observer algorithm allows not only the computation of the rotor magnetic-flux phasor position and rotor angular speed but also parameter estimation using (67)–(69). If the motor inductances are known, it should be possible to compute rotor resistance using (12) or (13) and stator resistance from (11). Simulation experiments proved that it is really possible to estimate stator resistance $R_{\rm s}$, but not the rotor resistance $R_{\rm r}$. The reason is very simple and can be shown using the original ac induction-motor model equation (2). The magnitude of the rotor magnetic-flux phasor is held constant during normal drive operation. In consequence, the rotor current phasor $\boldsymbol{i}_{\rm r}$ is orthogonal to the rotor magnetic-flux phasor $\boldsymbol{\Psi}_{\rm r}$. Equation (2) can be then rewritten into the form

$$\frac{d\boldsymbol{\Psi}_{\rm r}}{dt} = j\boldsymbol{\Psi}_{\rm r}\left(z_{\rm p}\omega + R_{\rm r}\frac{|\boldsymbol{i}_{\rm r}|}{|\boldsymbol{\Psi}_{\rm r}|}\right). \tag{70}$$

It is clear that if any difference between measured and estimated stator current is detected, it is not possible to determine whether the difference is caused by a change in ω or in $R_{\rm r}$. Only the value of the complete term $z_{\rm p}\omega + R_{\rm r}(|\boldsymbol{i}_{\rm r}|/|\boldsymbol{\Psi}_{\rm r}|)$ can be estimated. We have to know either rotor angular velocity or rotor resistance and then it is possible to compute the other variable. Although there is a possibility off addition of some variations to the rotor magnetic flux (e.g., sinusoidal or square wave changes to rotor flux reference value) in such way that phasors $\boldsymbol{i}_{\rm r}$ and $\boldsymbol{\Psi}_{\rm r}$ will not be orthogonal, this method is practically unusable in many cases due to limitations in maximum available stator voltage. That is why it is necessary to find other methods for obtaining the value of the rotor resistance [8]. It leads to the practical result that observer parameters k_{ξ_2} and k_{ξ_3} should be set $k_{\xi_2} = k_{\xi_3} = 0$.

B. Observer-Gain Tuning

Proper observer-gain selection is one of the biggest difficulties in the speed-observer design. In applications, using an extended Kalman filter (EKF) as a speed observer, it is possible to tune observer gains automatically requiring knowledge of noise-signal statistical properties that are, unfortunately, not usually known [9]. The ac induction-model linearization is the other possibility and it allows us to study observer dynamics analytically [10], [11]. However, this approach is not perfect as it provides good results only in the case of slow rotor-speed changes as the rotor speed has to be considered to be constant and is useful especially for flux-observer tuning.

The proposed observer is a nonlinear system and it is very difficult to describe its dynamics analytically. That is why we have no general and automatic method for the observer-gain tuning at this time. However, it is possible to describe some guidelines for observer-gain tuning.

The Lyapunov function (32) must be a positive definite function and that is why we have to set gains $\{k_\omega, k_{\xi_1}, k_{\xi_2}, k_{\xi_3}\}$ to be positive. The observer-stability analysis leads to conclusion (37) and also, gains $\{k_1, k_2\}$ have to be positive. According to stability analysis, observer gains can have any positive value. Unfortunately, it is not true in practice. We have to keep observer computation demands as low as possible as we want to implement it on a relatively low-cost and low-performance controller. That is why only Euler's integration method should be used. Euler's integration can be inaccurate when performing calculations with high-frequency signals, which can occur as a result of setting the observer gains to high values.

Gains k_1 and k_2 have a direct impact on the observer stator-flux tracking ability. It is especially clear that k_1 should be set as high as possible (the highest possible value before numerical instability occurs can be determined experimentally) as it determines the time constant of exponential stator-current error convergence (28).

The observer-parameter adaptation can be tuned by gains k_{ξ_1}, k_{ξ_2}, and k_{ξ_3}. It has been shown earlier that it is not usually possible to estimate rotor resistance by the presented algorithm. As we have to use some other method for obtaining the rotor-resistance value, it is advisable to assume that $\Delta\xi_2 = \Delta\xi_3 = 0$ and set $k_{\xi_2} = k_{\xi_3} = 0$. The gain k_{ξ_1} should be set with respect to the drive thermal dynamics; the higher value it has, the faster stator-resistance changes due to temperature changes can be tracked.

The last gain k_ω represents speed-tracking dynamics. A higher value can improve rotor-speed-change tracking. On the other hand, a high value of k_ω can cause poor performance in the low-speed region when speed information in the stator voltage and current measurement disappears, and the observer is then influenced mostly by noise signals.

C. Dead-Time Compensation

Knowledge of accurate values of stator current and stator voltage is essential for correct speed-observer operation. While the stator current is measured using current sensors, we suppose that the stator-voltage value is known as it is the control system output variable. Unfortunately, a significant difference between the output of the control system and the actual voltage passed to the drive can be present.

In most cases, the stator voltage is generated using pulsewidth modulation (PWM), which controls complementary transistor switching in a bridge circuit. The transistors should be switched complementarily. Simultaneously switching both transistors ON would cause a short-circuit connection, resulting in damage to power electronics. That is why a short "dead time" when both transistors are switched OFF is inserted into the switching cycle. During the dead-time duration, the load inductance defines the voltage to keep inductive current flowing through diodes. The actual stator voltage then depends on the current direction.

This difference is not too important for the control algorithm itself as it can be usually compensated by a current controller. However, if we use a model-based flux and speed observer, it is necessary to assure the stator voltage put on the motor is the same as the voltage used in the model computation.

The simplest method of solving this problem is based on actual stator-voltage measurement [12]. This is probably the best method as it can provide an accurate stator-voltage value and help to achieve significant improvement in the observer performance. On the other hand, we have to use some additional voltage-measurement hardware in this case. As we are trying to maintain hardware simplicity, we do not like to use another voltage sensor, and that is why we do not use this method.

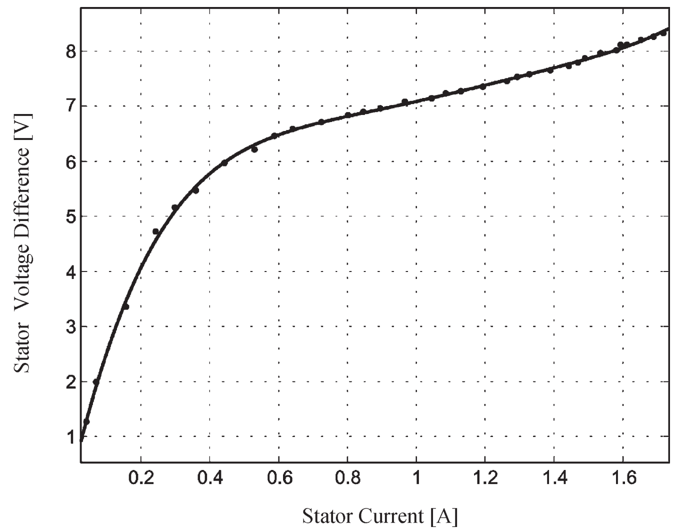

Fig. 2. Stator-voltage error.

Another method is based on sensing stator-current direction and changing PWM signal's pulsewidth to achieve desired stator voltage. This method supposes that the stator-voltage error is constant and depends only on stator-current direction. Functions supporting the constant-compensation method are directly implemented on Freescale hybrid controllers (former Motorola DSPs) [13] but additional current-direction components (comparators) are required.

In our algorithm, we use a more precise method. The difference in stator voltage is not constant, but depends on stator-voltage current value. We have measured the dependence of stator-voltage error and stator current, as is shown in Fig. 2. It is possible to find a suitable interpolation formula (in our case, fifth-order polynomial for low current and linear function for high current) and use it for dead-time-compensation calculation on DSP in real time. The calculated compensation is added to the desired stator-voltage value passed to the PWM subsystem. The compensated voltage is then both present on the machine stator winding and also used in observer calculation.

The dead-time compensation is very important especially at the low-speed region when stator voltage is usually low and the relative stator-voltage error can become very significant. This compensation allows our control system to be working at speeds even as low as 20 r/min.

III. Algorithm Implementation

A. Simulation

In the first step, the algorithm was simulated in the control structure using field-oriented-control based on rotor flux [14]. The simulation was carried out completely in a Matlab Simulink environment. In the second step, the observer algorithm has been implemented on the Freescale 56F805 hybrid controller chip (former Motorola DSP56F805). The simulation was then done in a hybrid environment where the ac induction motor was simulated using Matlab Simulink while the

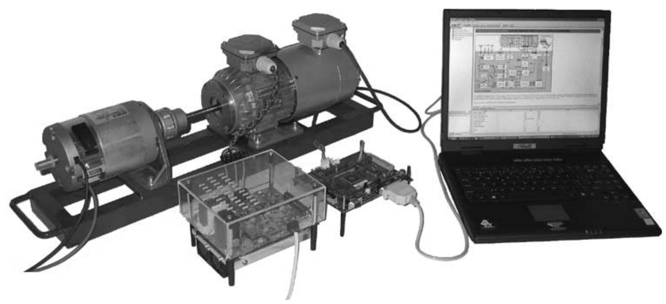

Fig. 3. Experimental system.

complete motor-control algorithm including the observer ran on the DSP. The simulation results proved the algorithm ability of the magnetic-flux phasor-position estimation and rotor-speed tracking [15].

B. Hardware Implementation

The algorithm was also tested on the real ac induction machine using our experimental system shown in Fig. 3. A small 250-W induction machine with two pole pairs was used with approximate parameter values $R_{\mathrm{s}} = 32\ \Omega$, $R_{\mathrm{r}} = 22\ \Omega$, $L_{\mathrm{s}} = 0.85$ H, $L_{\mathrm{r}} = 0.85$ H, and $L_{\mathrm{m}} = 0.7$ H. The load torque was produced by a dc permanent-magnet motor mechanically connected to the induction machine. The observer was implemented on the Freescale 56F805 hybrid controller evaluation board together with the complete control system based on the rotor-flux-oriented vector-control algorithm [14]. The Freescale 56F805 hybrid controller chip is equipped with peripherals needed to control electrical drives, and also, the evaluation board is suitable for motor-control-application testing. The Freescale three-phase ac high-voltage brushless dc power stage has been used to supply control signals to the machine.

IV. Results

In the first experiment, the ability of speed-change tracking was studied. The motor was running without any load. Observer parameters were tuned experimentally to values $k_1 = 2$, $k_2 = 300$, $k_\omega = 8000$, $k_{\xi_1} = 2000$, $k_{\xi_2} = 0$, and $k_{\xi_3} = 0$. The algorithm was able to track the rotor-speed changes without significant error even in the case of rapid speed change. The comparison of real and estimated rotor speed is shown in Fig. 4. In some cases, quite a big error in the estimated speed in the very-low-speed region can occur. This effect can occur during machine startup and also during speed reversal. This error is caused by two reasons.

The first one is the well-known fact that the speed information contained in stator voltage and current measurement disappears as the synchronous stator frequency goes to 0 [10], affecting the model-based speed observer's performance in the low-speed region. It is possible to overcome this problem by using a field-weakening algorithm to achieve a higher stator field frequency.

The other reason for the speed-estimation error in the low-speed region lays in the imperfect dead-time compensation. In the low-speed region, the stator voltage is low. On the other hand, the stator current can be high during acceleration from zero speed or during speed reversal. This is the situation when the relative stator-voltage error caused by PWM dead time reaches its maximal value. Although we have tried to introduce the dead-time-compensation algorithm, there is still a slight difference between the real stator voltage and its value used in the observer calculation in the low-voltage region. It is possible to overcome this problem effectively by direct stator-voltage measurement [12], increasing the used hardware cost.

The relative speed-estimation error $\delta_\omega = (\omega - \tilde{\omega}/\omega)100$ is shown in Fig. 5. The complete speed range has been evaluated for the machine without external load torque (only friction torque is present), while an experiment with the load torque fixed at 0.5 N·m has been made only for a limited speed range. At this time, we are not able to control constant load torque at a rotor speed under 500 r/min and we cannot run the induction machine at speeds over 1600 r/min, producing higher torque, because of power limitation. We can see that the algorithm can

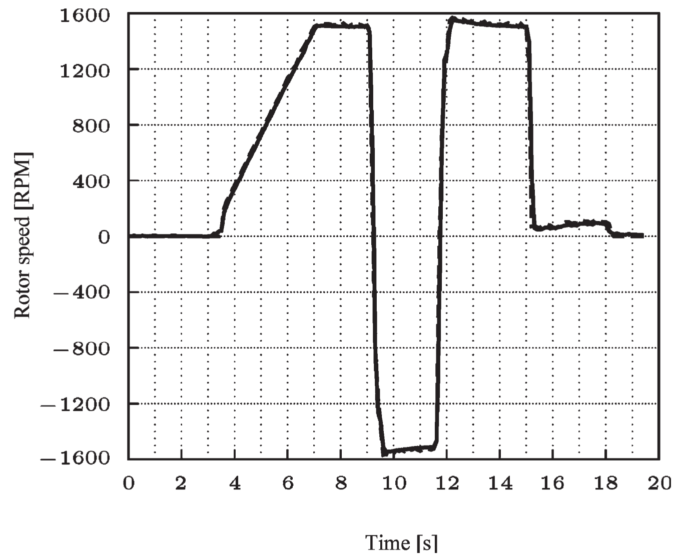

Fig. 4. Comparison of real rotor speed (dashed) and estimated value (solid).

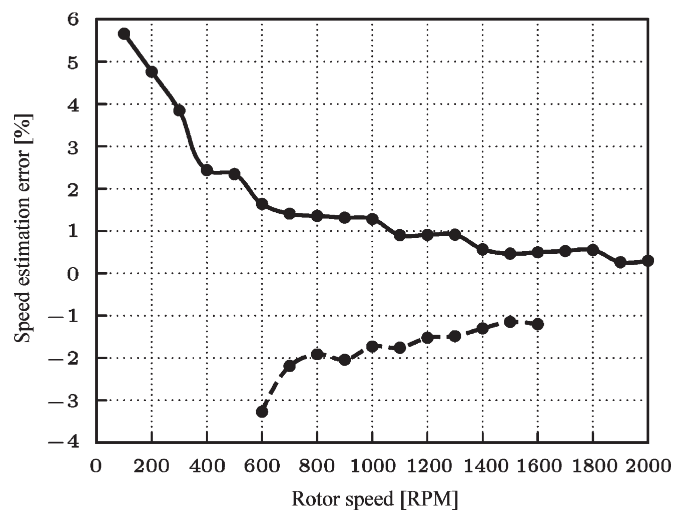

Fig. 5. Estimated speed relative error for no load (solid) and load torque 0.5 N·m (dashed).

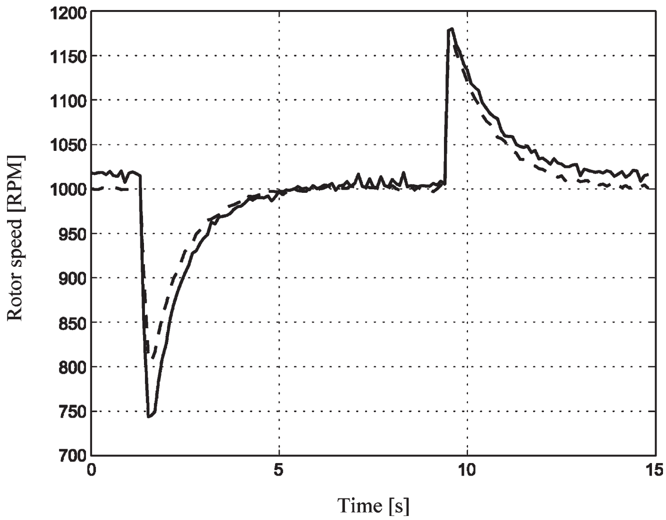

Fig. 6. Comparison of real rotor speed (dashed) and estimated value (solid) during load-torque change.

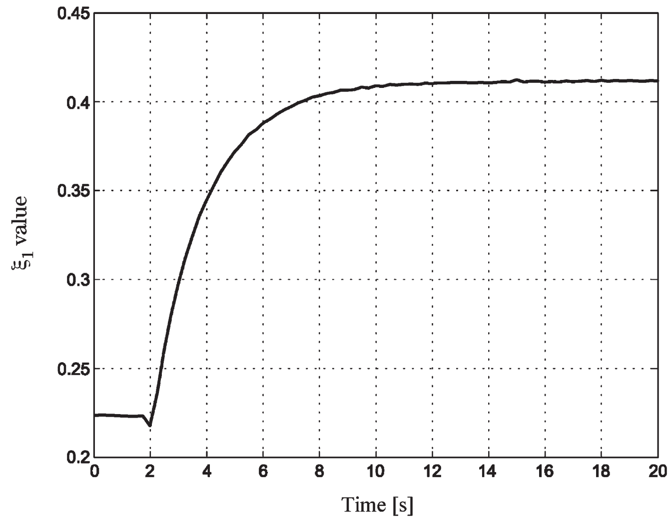

Fig. 7. ξ_1-parameter adaptation.

achieve a speed-estimation error lower than 2% at speeds higher than 1000 r/min. This precision is satisfactory for common ac induction-machine applications. Both curves in Fig. 5 have the shape of a hyperbolic function. The main reason of the speed-estimation steady-state error is the difference between the real rotor resistance and its value used in the observer calculation. It can be shown that if we keep the load torque constant, the rotor current $|\boldsymbol{i}_{\mathrm{r}}|$ is also constant. From (70), it is clear that if the speed-estimation error is caused by inaccurate rotor-resistance knowledge, then the absolute value of the speed-estimate error is constant and the relative error will be a hyperbolic function of the rotor speed. The relative error is positive for the machine running without load as the machine temperature is relatively low and the real rotor resistance is lower than the fixed rotor-resistance value used in the observer calculation. On the other hand, the relative speed error for the machine running under high load is negative as the machine temperature becomes high, resulting in the higher real rotor resistance. Based on Fig. 5, we can make the conclusion that the main reason for the speed-estimate error in the proposed algorithm is the rotor-resistance error.

The next experiment was aimed to examine observer behavior during load-torque change. The motor has started its operation with zero load torque. Then, the load-torque change to 1 N·m was introduced at time 2 s, and the load torque returned to 0 at time 9 s. As it can be seen in Fig. 6, the rotor speed changed for a short time until the control algorithm compensated the load torque. However, even in this situation, there is only a little error in the speed estimate. The load torque causes a motor-temperature increase and, in consequence, motor-parameter changes. The observer algorithm then tries to adapt the ξ_1 parameter, as can be seen in Fig. 7.

If high load torque is applied for a long time period, the motor temperature increases significantly. In this situation, the real value of the rotor resistance can differ from the model value and it can lead to error in rotor-speed estimate, as is shown in Fig. 8, where maximum possible load torque was applied to the drive for a long time. The drive was able to continue in normal operation at a slightly different speed as the error in rotor-resistance value has no impact on the magnetic-flux phasor-position estimation.

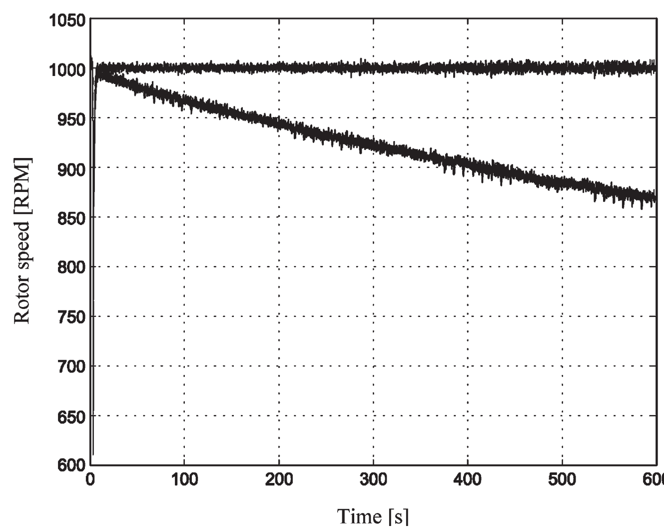

Fig. 8. Comparison of real rotor speed and estimated value at high-temperature condition.

V. Conclusion and Future Work

A. Conclusion

The presented speed-observer algorithm has been tested on a real ac induction machine. The algorithm has been implemented on a Freescale 56F805 hybrid controller chip that is suitable for motor-control applications. The observer algorithm seems to be time efficient as it is possible to compute it on the DSP in 20 μs. As was shown, the algorithm is able to track the rotor speed even in the case of rapid torque change. The presented results have been obtained in testing on a real ac induction machine controlled by classical rotor-flux-oriented vector control [14]. As the algorithm does not depend on the control scheme, it is possible to use it with other ac induction-machine-control algorithms like direct torque control (DTC) or predictive direct stator flux control (PDSFC) [16].

It was shown that the correct knowledge of the rotor-resistance value is essential for accurate rotor-speed estimation. Although many authors of articles and application notes on sensorless control do not mention it, changes of rotor-resistance value due to temperature changes can lead to a significant error in rotor-speed computation.

Dead-time compensation should be considered as the dead time introduced as a safety mechanism to protect switching parts of the power circuit can cause a difference between the real stator voltage and the stator voltage used by the control algorithm. If the wrong supposed stator-voltage value is used as a motor model input, the results may be unpredictable.

B. Future Work

Future research will concentrate on methods of the rotor-resistance estimation and dead-time compensation. In consequence, we will be able to use more accurate values of motor parameters during speed-observer computation and improve its performance. The research will be aimed especially to the ac induction-machine temperature models [17], [18]. We suppose that knowledge of the drive temperature conditions will allow us to develop better parameter-estimation algorithms.

Speed estimation based on rotor-slot harmonics will be also studied [19]. Algorithms based on rotor-slot harmonics can provide a mechanical rotor-speed estimate even in the case when electrical parameters of the drive are not known. The problem is that these algorithms are difficult to use as the only speed-estimation algorithm. We will try to develop an algorithm based on the observer proposed in this article coupled with the speed estimation using rotor-slot harmonics. We suppose that we will be able to achieve good performance in a wide speed range together with the parameter-adaptation ability.

REFERENCES

[1] J. Holtz, "Sensorless speed and position control of induction motors," in *Proc. 27th Annu. Conf. IEEE Industrial Electronics Society (IECON)*, Denver, CO, 2001, pp. 1547–1562.

[2] ——, "Sensorless control of induction motor drives," *Proc. IEEE*, vol. 90, no. 8, pp. 1359–1394, Aug. 2002.

[3] K. Rajashekara, A. Kawamura, and K. Matsuse, *Sensorless Control of AC Motor Drives*. Piscataway, NJ: IEEE Press, 1996.

[4] M. Barut, S. Bogosyan, and M. Gokasan, "Speed sensorless direct torque control of IMS with rotor resistance estimation," *Energy Convers. Manage.*, vol. 46, no. 3, pp. 335–349, Feb. 2005.

[5] G. Welch and G. Bishop, "An introduction to the Kalman filter," in *Proc. Special Interest Group Graphics (SIGGRAPH) Course Syllabus*, Los Angeles, CA, 2001, p. 82.

[6] P. Vaclavek, P. Blaha, and J. Lepka, "State observer for sensorless AC induction motor control, Kalman filter versus deterministic approach," in *Proc. 11th Int. Workshop Robotics Alpe-Adria-Danube Region (RAAD)*, Balatonfüred, Hungary, 2002, pp. 353–358.

[7] J. Zamora and A. Garcia-Cerrada, "Online estimation of the stator parameters in an induction motor using only voltage and current measurements," *IEEE Trans. Ind. Appl.*, vol. 36, no. 3, pp. 805–816, May/Jun. 2000.

[8] J. Faiz and M. Sharifian, "Different techniques for real time estimation of an induction motor rotor resistance in sensorless direct torque control for electric vehicle," *IEEE Trans. Energy Convers.*, vol. 16, no. 1, pp. 104–109, Mar. 2001.

[9] K. Shi, T. Chan, Y. Wong, and S. Ho, "Speed estimation of an induction motor drive using an optimized extended Kalman filter," *IEEE Trans. Ind. Electron.*, vol. 49, no. 1, pp. 124–133, Feb. 2002.

[10] B. Peterson, "Induction machine speed estimation, observations on observers," Ph.D. dissertation, Dept. Ind. Elect. Eng. Autom., Lund Inst. Technol., Lund, Sweden, 1996.

[11] H. Kubota, K. Matsuse, and T. Nakano, "DSP-based speed adaptive flux observer of induction motor," *IEEE Trans. Ind. Appl.*, vol. 29, no. 2, pp. 344–348, Mar./Apr. 1993.

[12] G. Edelbaher, E. Urlep, M. Curkovic, and V. Kranjec, "Low speed performance improvement in sensorless drive using measured stator voltages of PWM Voltage Source Inverter," in *Proc. IEEE Int. Conf. Industrial Technology*, Maribor, Slovenia, 2003, pp. 542–547.

[13] R. Visinka, "3-phase AC induction motor drive with dead time distortion correction reference design," in *Designer Reference Manual DRM019/D*. Austin, TX: Freescale Semiconductor, Inc., 2003.

[14] J. Lepka, "3-phase AC induction motor vector control using 56F805," in *Designer Reference Manual DRM023/D*. Austin, TX: Freescale Semiconductor, Inc., 2003.

[15] P. Vaclavek and P. Blaha, "State observer for sensorless ac induction motor control and parameters estimation," in *Proc. 12th Int. Workshop Robotics Alpe-Adria-Danube Region (RAAD)*, Cassino, Italy, 2003, CD-ROM.

[16] P. Blaha and P. Vaclavek, "A practical realization of PDSFC algorithm using Motorola dsp56f80x," in *Proc. IEEE Int. Conf. Industrial Technology*, Maribor, Slovenia, 2003, pp. 554–559.

[17] B. Bose and N. Patel, "Quasi-fuzzy estimation of stator resistance of induction motor," *IEEE Trans. Power Electron.*, vol. 13, no. 3, pp. 401–409, May 1998.

[18] C. Kral, T. Habetler, R. Harley, F. Pirker, G. Pascoli, H. Oberguggenberger, and C.-J. Fenz, "Rotor temperature estimation of squirrel-cage induction motors by means of a combined scheme of parameter estimation and a thermal equivalent model," *IEEE Trans. Ind. Appl.*, vol. 40, no. 4, pp. 1049–1057, Jul./Aug. 2004.

[19] S. Nandi, S. Ahmed, and H. Toliyat, "Detection of rotor slot and other eccentricity related harmonics in a three phase induction motor with different rotor cages," *IEEE Trans. Energy Convers.*, vol. 16, no. 3, pp. 253–260, Sep. 2001.

Pavel Vaclavek (M'04) received the M.Sc. and Ph.D. degrees in cybernetics from Brno University of Technology, Brno, Czech Republic, in 1993 and 2001, respectively. He also received the M.Sc. degree in industrial management from the same university, in 1998.

He is with the Centre for Applied Cybernetics, Brno University of Technology. His research interests include speed sensorless control of induction machines, system modeling, and parameter estimation.

Petr Blaha received the M.Sc. and Ph.D. degrees in cybernetics from Brno University of Technology, Brno, Czech Republic, in 1996 and 2001, respectively.

He is with the Centre for Applied Cybernetics, Brno University of Technology. His research interests include speed-sensorless control of induction machines, parameter estimation, and polynomial methods in control systems.